KASDI MERBAH UNIVERSITY – OUARGLA

FACULTY OF HYDROCARBONS, RENEWABLE ENERGIES, AND EARTH & UNIVERSE SCIENCES

DEPARTMENT OF EARTH AND UNIVERSE SCIENCES

Academic Master's Thesis

Field of Study: Earth and Universe Sciences

Specialization: Sedimentary Basin Geology

Topic

Mineralogical And Geotechnical Characterization Of Temassine Clays From The Touggourt Region, Algeria"

Presented by:

Meridji Mohammed Kamel-Eddine

Publicly defended on:

Jury Members:

Name		Institution	Grade
BENKHELIFA Randa	Mme	UKM Ouargla	MCB
BELKSEIR Mohamed Saleh	Mr	UKM Ouargla	Pr
CHEMAM Asma	Mme	UKM Ouargla	MCB
SATOUH ADEL	Mr	UKM Ouargla	MCA

Academic Year: 2025/2026

Abstract

This study concerns the characterization of clays from the Timassine region in Touggourt, northeastern Sahara of Algeria. The study area belongs to the Saharan platform and is marked by Quaternary deposits of sands, clays, and gypsum formed in lacustrine environments during the drying of lagoons and chotts. Several laboratory methods were applied, including mineralogical, granulometric, chemical, and geotechnical analyses, to describe the nature of these materials and evaluate their potential use in construction.

Keywords: Timassine clays, , characterization, granulometry, mineralogy, geotechnical analysis, Touggourt

ملخص

تختص هذه الدراسة بتوصيف الطين في منطقة تيماسين بولاية تقرت شمال شرق الصحراء الجزائرية. المنطقة المدروسة جزء من المنصة الصحراوية وتتميز بترسيبات رباعية من الرمال والطين والجبس، تكونت في بيئة بحيرية أثناء مرحلة جفاف البحيرات والسبخات. تم استخدام عدة طرق مخبرية، منها التحليل المعدني، والتحليل الحجمي، والتحليل الكيميائي .والجيوتقني، لوصف طبيعة هذه المواد وتقييم إمكانية استعمالها في مجال البناء

الكلمات المفتاحية : طين تيماسين، تقرت، توصيف، التحليل الحجمي، علم المعادن، التحليل الجيوتقني

Résumé

Cette étude concerne la caractérisation des argiles de la région de Timassine à Touggourt, située au nord-est du Sahara algérien. La zone étudiée appartient à la plateforme saharienne et présente des dépôts quaternaires de sables, d'argiles et de gypse formés en milieu lacustre lors de la phase d'assèchement des lagunes et des chotts. Plusieurs méthodes de laboratoire ont été utilisées, notamment des analyses minéralogiques, granulométriques, chimiques et géotechniques, afin de décrire la nature de ces matériaux et d'évaluer leur potentiel d'utilisation dans la construction.

Mots-clés : Argiles de Timassine, Touggourt, caractérisation, granulométrie, minéralogie, analyse géotechnique

Acknowledgements

In the Name of Allah, the Most Gracious, the Most Merciful,
First and foremost, I would like to thank God for granting me the health, strength, and perseverance needed to accomplish this work.
I would also like to express my deep gratitude to all my teachers, from primary school to university, whose guidance and support have played a fundamental role in shaping our academic journey.
We extend our sincere appreciation to our supervisor, Dr. Chemam, for her valuable guidance, constructive feedback, and continuous support throughout the development of this work. Her expertise and encouragement were essential in making this achievement possible.
I extend my deepest thanks to Pr Mohamed saleh Belkseir for serving as examiner of this work, and to Dr. Randa Benkhelifa for chairing the committee, for their thoughtful evaluation, constructive feedback, and appreciated support throughout this academic endeavor.
Finally, I would like to acknowledge my own commitment, sacrifices, and determination to keep moving forward despite challenges. This work stands as a reflection of my dedication and perseverance.

Meridji Med Kamel-Eddine

Dedication

This dissertation is dedicated with deep love and gratitude to my parents, whose sacrifices and constant support have been the foundation of my life. You believed in me when I doubted myself, and your encouragement gave me the strength to continue. Every success I celebrate today is also your success, because it reflects your care, patience, and faith in me.

To my sisters, whose wisdom and gentle guidance helped me face challenges with courage. You taught me that perseverance is not only about working hard, but also about keeping dignity and hope in difficult times. Your advice has shaped my values and reminded me that true achievement is measured not only in results but in the way we live and respect others.

To my best friends, whose inspiration and mentorship opened my mind to new ideas. You showed me that knowledge is more than facts; it is a journey of discovery and responsibility. Your example has encouraged me to use what I have learned not only for myself but also to help others and contribute to society.

And to all teachers, colleagues, and friends who shared their time, advice, and encouragement, I thank you sincerely. Each of you has contributed in some way to this work, whether through guidance, discussion, or simple words of support.

This dissertation is not only the result of my effort, but also a reflection of the love, patience, and faith of those who walked with me. It is a symbol of gratitude to everyone who believed in me and helped me reach this goal. Without your presence and support, this achievement would have remained only a dream.

-Kamel

TABLE OF CONTENTS

LIST OF FIGURES

LIST OF TABLES

GENERAL INTRODUCTION

1.Context and Scientific Background

Clay minerals represent one of the most fundamental and ubiquitous constituents of the Earth's surface environment. Their fine-grained nature, layered phyllosilicate structures, and distinctive physical and chemical properties position them at the intersection of natural geological processes and a wide spectrum of human applications. From the earliest civilizations that exploited clay for pottery, bricks, and pigments, to contemporary industries that utilize clays in ceramics, drilling muds, paper production, pharmaceutical formulations, and environmental remediation, the scientific and economic relevance of these materials has remained constant across geological time and human history.

In the earth sciences, clay minerals are far more than sedimentary constituents; they are geochemical archives that encode the history of weathering, diagenesis, and basin evolution. Their mineral assemblages function as reliable indicators of paleoclimate, depositional environments, and post-depositional transformations. In engineering geology, clays are equally critical: their shrink-swell behaviour, plasticity, and low hydraulic conductivity exert a direct influence on soil mechanics, foundation stability, and the performance of construction materials. The study of clay minerals is therefore inherently interdisciplinary, bridging sedimentary geology, soil science, geotechnical engineering, industrial mineralogy, and environmental science.

2,Definition and Classification of Clay Minerals

The term "clay" encompasses both a textural and a mineralogical dimension that requires careful distinction. From a granulometric standpoint, clay designates particles smaller than 2 micrometers (μm) in diameter a size threshold below which particles exhibit unique physical behaviours, including plasticity when wet and cohesion when dry, which differentiate them from silt and sand fractions. However, particle size alone is insufficient to define clay minerals, since non-clay phases such as fine quartz or iron oxides may occur in the clay fraction without possessing the characteristic crystal-chemical properties of true clay minerals (Grim, 1968; Moore and Reynolds, 1997).

Mineralogically, clays are defined as a group of phyllosilicate minerals characterized by a layered crystal structure composed of tetrahedral sheets of silica (SiO_2) and octahedral sheets of alumina (Al_2O_3) or magnesia (MgO), arranged in different stacking configurations. These structural arrangements produce four principal mineral groups: kaolinite (1:1 layer structure), smectite and illite (2:1 layer structure), and chlorite (2:1 layer with an additional brucite-like interlayer). Each group displays distinct physical and chemical behaviour that is directly governed by its crystal architecture (Bergaya et al., 2006; Deer et al., 2013).

Kaolinite, characterized by strong interlayer hydrogen bonding, is non-expanding, thermally stable, and widely exploited in ceramics and paper production. Smectite (montmorillonite, bentonite) exhibits high swelling capacity and a very high cation exchange capacity (CEC) due to its expandable interlayers, making it critical in drilling muds and

environmental barrier systems. Illite, stabilized by potassium ions in the interlayer, is non-expanding and serves as a key indicator of burial diagenesis in sedimentary basins. Chlorite, enriched in magnesium and iron, is characteristic of low-grade metamorphic and hydrothermal environments (Chamley, 1989; Bergaya et al., 2006).

3,Genesis of Clay Minerals

The formation of clay minerals is a complex process governed by the interaction of geological, climatic, and geochemical factors. Clays may originate through three principal pathways: (i) chemical weathering of pre-existing silicate minerals, (ii) hydrothermal alteration by circulating hot fluids, and (iii) diagenetic transformation during burial in sedimentary basins (Chamley, 1989).

Chemical weathering is the most prevalent genesis pathway, involving the hydrolysis and leaching of feldspars, micas, and amphiboles. The resulting mineral assemblage is strongly climate-dependent: intense leaching in humid tropical environments favours kaolinite formation; semi-arid and alkaline conditions promote smectite; and temperate or marine settings commonly yield illite (Grim, 1968; Moore and Reynolds, 1997). Hydrothermal alteration, in contrast, produces montmorillonite, chlorite, or mixed-layer clays through fluid-rock interaction at elevated temperatures, commonly associated with volcanic or magmatic systems.

In sedimentary basins, diagenetic transformations exert a fundamental control on clay mineral assemblages during burial and compaction. The smectite-to-illite transition, occurring at burial depths of 2–4 km, involves the progressive incorporation of potassium into smectite interlayers, releasing water and altering reservoir properties. This transformation is of particular significance in petroleum geology, where it governs porosity evolution, fluid migration, and hydrocarbon trap integrity (Bergaya et al., 2006).

4.Physical and Chemical Properties

The physical properties of clay minerals derive directly from their fine particle size, layered crystal structure, and the presence of water in interlayer positions. Plasticity the most distinctive property of clay refers to the ability of water-saturated clay to be moulded and to retain its shape upon drying. This property arises from the adsorption of water molecules onto mineral surfaces, which act as lubricants between particles, and is quantitatively assessed through Atterberg limits (liquid limit, plastic limit, and plasticity index). Smectites exhibit the highest plasticity, while kaolinite shows comparatively lower values (Mitchell and Soga, 2005).

The shrink-swell behaviour of clays, particularly pronounced in smectite-group minerals, constitutes a major geotechnical hazard in construction and infrastructure. Volume changes induced by wetting and drying cycles generate expansive pressures capable of causing foundation failure, pavement damage, and structural cracking in buildings. Low hydraulic conductivity, on the other hand, renders clay-rich formations effective aquitards and cap rocks in hydrocarbon traps, as well as engineered barriers in waste containment systems (Bergaya et al., 2006; Mitchell and Soga, 2005).

Among the chemical properties of clays, cation exchange capacity (CEC) is particularly significant. It reflects the ability of clay surfaces and interlayers to adsorb and release cations, governing soil fertility, pollutant retention, and fluid-rock interactions in sedimentary basins. Specific surface areas in smectites can exceed 100 m^2/g, enabling strong adsorption of water, organic molecules, and heavy metals. The pH-buffering capacity of clays further contributes to geochemical stability in soils and sedimentary environments (Chamley, 1989; Grim, 1968).

5.Clays in Industrial and Construction Applications

The industrial exploitation of clay minerals spans a remarkably broad range of sectors. In the construction industry, clays are the primary raw material for the production of fired bricks, tiles, and ceramics. Their plasticity enables moulding into complex shapes, while their thermal behaviour during firing encompassing dehydroxylation, vitrification, and sintering produces durable, mechanically resistant products. The quality of fired clay products depends critically on mineralogical composition: the relative proportions of kaolinite, illite, and quartz govern shrinkage, porosity, compressive strength, and colour development (Dondi et al., 1997).

However, specific chemical constituents can significantly compromise the quality of fired clay products. Elevated concentrations of soluble sulfates (SO_4^{2-}) promote efflorescence and subflorescence on brick surfaces, while excess calcium carbonate ($CaCO_3$) when decomposed to free lime (CaO) during firing causes destructive post-firing expansion upon atmospheric moisture uptake. These chemical constraints must be rigorously assessed in the characterization of raw materials for brick production, particularly in arid and semi-arid regions where evaporitic diagenesis enriches subsurface clays in sulfate and carbonate phases (Cultrone et al., 2004; Dondi et al., 1997).

Beyond construction, clay minerals find extensive application in drilling technology (bentonite-based muds), environmental engineering (landfill liners, heavy metal immobilization), pharmaceutical formulations (gastrointestinal adsorbents, tablet excipients), and catalysis (acid-activated smectites). Their versatility derives from the interplay between crystal structure, surface chemistry, and response to thermal and chemical treatment (Bergaya et al., 2006).

Geological and Geotechnical Context of the Study Area

The Timassine–Touggourt region, located in the northeastern Sahara sedimentary basin (Oued Righ), provides a relevant and challenging geological context for clay characterization. The local geology reflects a long and complex stratigraphic history, ranging from Precambrian basement to Quaternary continental deposits. The most significant formations for the present study are the Mio-Plio-Quaternary continental deposits (Continental Terminal), which host intercalated clay horizons within sandy sequences, and the Cretaceous units particularly the Cenomanian and Senonian which contain evaporitic and carbonate-rich clay assemblages (Busson, 1972; Fabre, 1976).

The semi-arid to arid climate of the region, combined with the evaporitic character of the Saharan subsoil, imparts distinctive geochemical signatures to local clays. The pervasive

enrichment in sulfate minerals (gypsum, anhydrite) and calcium carbonate reflects the diagenetic history of the Saharan continental sequences, making the physicochemical assessment of these materials a prerequisite for any construction application. Furthermore, the scarcity of conventional building materials in this region elevates the economic and strategic importance of identifying locally available resources suitable for fired brick production.

The clay deposits of Timassine are predominantly associated with Quaternary alluvial and lacustrine environments along the Oued Righ valley. Field sampling has identified four distinct clay facies red, green (two varieties), and yellow whose macroscopic differences suggest compositional and mineralogical variability. This diversity provides a scientifically productive framework for comparative characterization, allowing the influence of grain size, mineralogy, and geochemistry on physical and geotechnical properties to be systematically evaluated (Chamley, 1989; Mitchell and Soga, 2005).

6. Objectives and Structure of the Present Study

This Master's thesis aims to provide a comprehensive characterization of four clay samples collected from the Timassine region, Wilaya de Tougourt, southeastern Algeria, with the dual objective of contributing to the scientific understanding of Saharan clay deposits and evaluating their potential for use as construction materials, particularly in fired brick production. The study integrates geological, mineralogical, granulometric, physicochemical, and geotechnical analyses to develop a multi-faceted assessment of the sampled materials.

The work is organized into three chapters. Chapter I establishes the geological and lithostratigraphic framework of the Touggourt–Timassine area, providing the regional and local context necessary for the interpretation of laboratory results. It reviews the principal sedimentary units from the Paleozoic to the Quaternary, with emphasis on the formations relevant to the sampled clay intervals. Chapter II presents a systematic review of clay minerals encompassing their definition, genesis, typology, physical properties, chemical properties, and applications constituting the theoretical basis for the analytical programme. Chapter III reports and discusses the laboratory results, including X-ray diffraction (XRD) analysis, hydrometer sedimentation tests, chemical and physicochemical characterization (soluble salts, calcium carbonate, pH), bulk density measurements, and Atterberg limit determinations. The synthesis of these results permits a comprehensive geotechnical classification of the four clay varieties and a critical assessment of their suitability as raw materials for construction applications in the Saharan context.

By combining classical analytical techniques with a rigorous theoretical framework, this study seeks to fill a gap in the documentation of clay resources in the Oued Righ basin and to provide practical recommendations for the sustainable use of local geological materials in regional infrastructure development.

Chapter I. Geological Framework

I.1. Regional Geological Framework

The Timassin–Touggourt region belongs to the north-eastern Sahara sedimentary basin (Oued Righ). The geology consists of several superimposed sedimentary layers. At the base, there are Precambrian rocks, which are very old igneous and metamorphic terrains. These are overlain by thousands of meters of sediments ranging from the Cambrian to the Quaternary.

The Paleozoic formations are mostly sandstones and shales, deposited in desert and periglacial conditions. Later, during the Triassic and Jurassic, the basin received thick deposits of sands, clays, and evaporites, forming what geologists call the **Continental Intercalaire** (Busson, 1972).

The Cretaceous is particularly significant as it marks a transition from marine to continental environments. Sands and clays (Fabre, 1976) dominate the Albian. The **Cenomanian** shows alternations of dolomites, limestones, clays, and evaporites, which make it largely impermeable (Bel & Cuche, 1969). The **Turonian** is a massive limestone and dolomite unit, very well defined in this basin. Above it, the **Senonian** displays two distinct facies: a lower lagoonal facies with clays and salts (low permeability), and an upper carbonate facies that is permeable (Busson, 1972).

The **Eocene** succession consists of dolomites and limestones, sometimes mixed with marls and evaporites, reaching thicknesses of 100–500 m (Bel & Cuche, 1969). Finally, the **Mio-Plio-Quaternary** deposits are continental, made of sands, clays, and gypsum. These are known as the **Continental Terminal**, and in Oued Righ they host two aquifer levels separated by a clay horizon (Bouzouada & Boussaid, 2018).

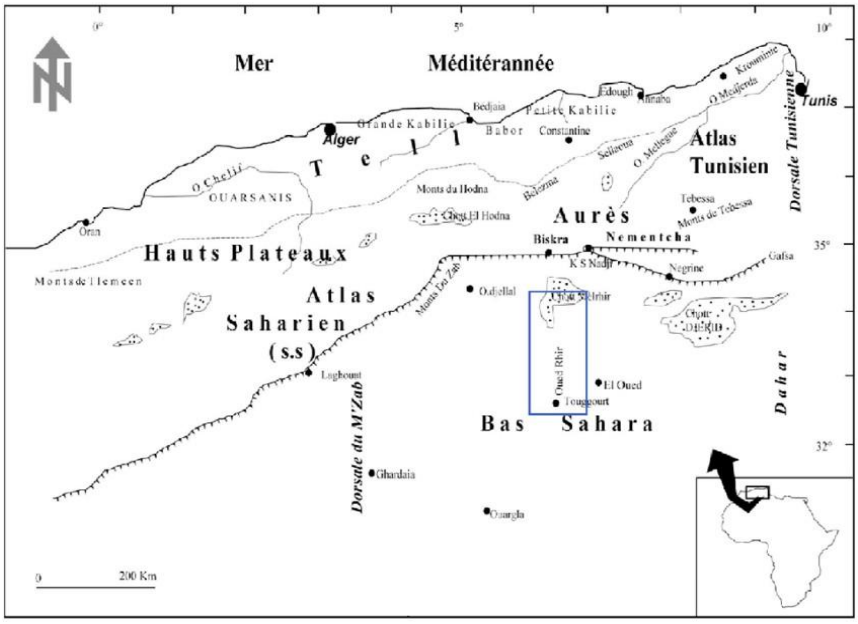

Figure 1 – Geographical situation of Oued Righ

I.2. Local Geological Framework

The Touggourt–Timassin area is part of the Saharan platform. The South Atlas Fault and the foothills of the Aurès mountains, to the south by the Tinrhert escarpment, to the east by the Cretaceous outcrops of Dahar, and to the west by the Mzab ridge, bound it to the north.

The geological map of Touggourt shows mainly Quaternary formations. These include recent dunes at Meggarine, Sidi Slimane, and Erg es-Sayah. There are also continental Quaternary deposits at Merdjadja, and modern alluvium at Timassin and Zaouïa. These deposits are significant as they represent the most recent geological episode in the valley and are directly related to the clay deposits investigated in Timassin.

I.3. Lithostratigraphy

In the Timassin–Touggourt area, the lithostratigraphy shows a clear succession of formations that reflect the geological history of the basin.

- Albian: This unit is predominantly composed of sands and clays, lying between the Aptian dolomites below and the Cenomanian clays above. It records the influx of large quantities of detrital sediments into the basin (Fabre, 1976).

- Vraconian: The Vraconian is a transitional stage between the sandy Albian and the clay-carbonate Cenomanian. It is represented by irregular alternations of clayey dolomites and sandy clays. In many boreholes, this stage is difficult to distinguish and is often confused with either Albian or Cenomanian deposits (Busson, 1972).

- Cenomanian: This formation is made of dolomites, dolomitic limestones, clays, and evaporites. The passage from Vraconian to Cenomanian is marked by the appearance of evaporites and dolomites. Its upper limit is defined by the massive limestones of the Turonian. The Cenomanian is largely impermeable due to the presence of evaporites (Bel & Cuche, 1969).

- Turonian: The Turonian is a thick unit of limestone and dolomite, very well defined in the Sahara basin. In the study area, its thickness ranges between 25 and 70 m, but it can exceed 300 m near the chotts. It is easily distinguished from the underlying Cenomanian clays and evaporites and the overlying Senonian deposits (Bel & Cuche, 1969).

- Senonian: This stage has two distinct facies. The lower Senonian is lagoonal, with clays, salts, and anhydrite, and exhibits very low permeability. The upper Senonian is carbonate, with permeable formations that contrast with the lower facies (Busson, 1972).

- Eocene: At the base, the Eocene is carbonate, composed of dolomites and limestones with some marls, clays, and evaporites. Its thickness varies between 100 and 500 m. At the top, the Eocene becomes evaporitic, with limestones, anhydrite, and marls, reaching about 100 m under the chotts (Bel & Cuche, 1969).

- Mio-Plio-Quaternary (Continental Terminal): These deposits are continental, made of sands, clays, and gypsum. In the Oued Righ valley, they host two aquifer levels within sandy layers, separated by a clay horizon. Above them lie the Plio-Quaternary lacustrine deposits, which are argillaceous, sandy, and gypsiferous, formed during the desiccation of lagoons and chotts (Bouzouada & Boussaid, 2018).

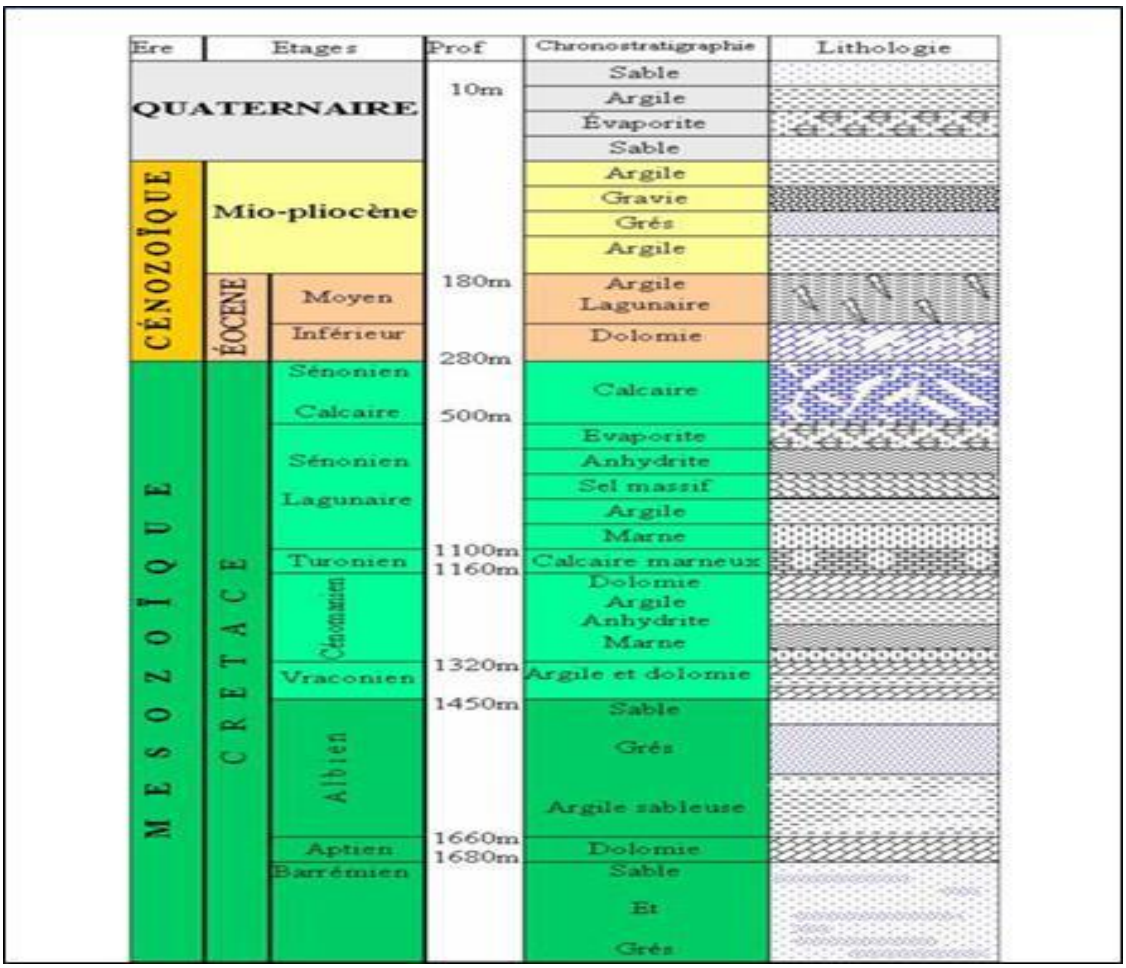

Figure 2 : Log stratigraphique synthétique de la région de Touggourt (Busson; 1972)

CHAPTER II. MATERIALS AND METHODS

Introduction

This chapter presents the experimental methods and laboratory techniques used to characterize the clay soils collected from the Timassine region, Wilaya of Tougourt. The study of fine-grained soils such as clays requires a combination of mineralogical, granulometric, and geotechnical analyses in order to fully understand their physical and mechanical behavior. To this end, three complementary methods were employed: X-ray diffraction (XRD) for the identification of clay minerals and phases, sedimentation (hydrometer) analysis for the determination of the particle size distribution of fine fractions, and the Atterberg limits test for the assessment of plasticity and consistency. The protocols followed in this study are consistent with standard laboratory procedures and relevant geotechnical norms.

II.1. The mineralogical Characterization

II.1.1 : X-Ray Diffraction (XRD)

The mineralogical analysis by X-ray diffraction (XRD) was carried out prior to observations under the binocular microscope. This analysis was performed at the Scientific Research Centre of the Earth Sciences University of Ouargla. The clay samples were first ground and reduced to fine powder (Fig. 4b), then placed into the sample holder (Fig. 4c) before being analyzed using a BTX-716 diffractometer (Fig. 4d). The mineralogical composition is subsequently obtained in the form of a diffraction pattern.

The operating principle of this technique is based on the interaction between a monochromatic X-ray beam and the crystal lattice of clay minerals. When this beam strikes the reticular planes of a mineral, it is diffracted according to **Bragg's Law**: $\mathbf{n\lambda = 2d \cdot \sin\theta}$ where n is the diffraction order, λ is the wavelength of the X-ray radiation, d is the interplanar spacing characteristic of the mineral, and θ is the angle of incidence. Each mineral possesses a unique set of d-spacings, producing a distinct diffraction pattern — a true crystallographic "fingerprint." The identification of mineral phases is then carried out by comparison with reference databases (JCPDS/ICDD).

In the case of clays, XRD makes it possible to identify clay minerals (kaolinite, illite, smectite, chlorite, etc.) as well as associated accessory minerals (quartz, calcite, feldspars, etc.), and to quantify their relative proportions within the sample.

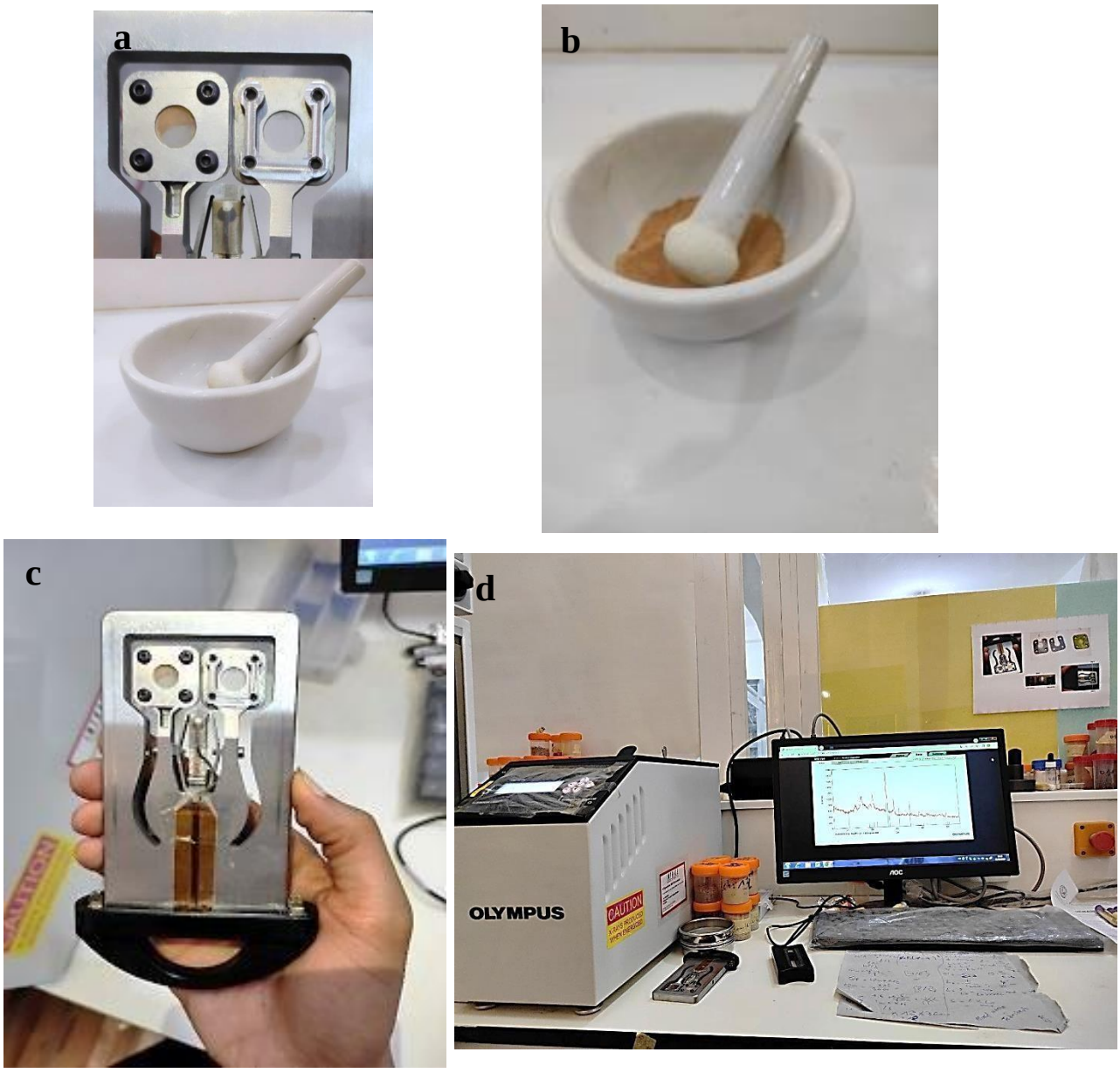

Figure 3: shows a) Sample preparation equipment b) Powdering of the sample c) Sample holder d) BTX-716 diffractometer apparatus.

II.2: Geotechnical Characterization of Four Clay Samples

In order to characterize the geotechnical properties of the studied clay materials, both the Atterberg limits test and the sedimentation (hydrometer) analysis were carried out on four clay samples collected from the study area.

II.2.1 : Sedimentation (Hydrometer) Analysis of Soils

The sedimentation granulometric analysis is a geotechnical test used to determine the weight distribution of fine soil particle sizes, applicable to natural soil elements passing through an 80 µm square-mesh sieve; particles smaller than 1 µm, however, cannot be differentiated by this method. This test complements sieve analysis and is essential for soil description and classification. Its principle is based on Stokes' law, which states that in a liquid medium at rest, the settling velocity of fine to very fine grains depends on their size establishing, for spherical grains of equal density, a direct relationship between grain diameter and sedimentation velocity applied by convention to determine equivalent particle diameters.

To carry out this analysis, the following equipment is required: a precision balance (accuracy: 1/1000 of the measured value), an 80 µm square-mesh sieve (diameter ≥ 250 mm), a non-alterable collection tray (60 × 40 × 12 cm), a drying oven adjustable to 105 °C and 50 °C, a mortar with soft-material pestle (diameter ≥ 20 cm), and a plunging-type mechanical stirrer adjustable up to 10,000 rpm with a container of minimum 600 cm^3 capacity. The sample is dispersed in a deflocculant solution prepared from 440 cm^3 of distilled water and 60 cm^3 of a 5% sodium hexametaphosphate solution ($Na_6(PO_3)_6 \cdot 10H_2O$), stored away from light for no more than one month, in order to prevent particle flocculation and ensure complete dispersion.

The prepared suspension is then transferred into two graduated transparent glass cylinders of minimum 2,500 cm^3 capacity and internal diameter of 85 ± 5 mm (Fig. 5a), where the turbidity of the suspension clearly reflects the high fine particle content of the clay samples. Before each density reading, the suspension is homogenised using a manual stirrer (Fig. 5c), whose shaft — 6 ± 1 mm in diameter and 601 ± 50 mm in total length — ensures effective mixing throughout the cylinder. The hydrometer (Fig. 5d), torpedo-shaped with a graduated stem ranging from 0.9950 to 1.0300 and a reading accuracy of 0.0005, is then carefully immersed into the suspension to measure its density at precise time intervals, as illustrated in Fig. 5b, where the instrument is visible inside the cylinder during the test. Temperature corrections are applied using two thermometers with an accuracy of 0.5 °C and an operating range of 10–35 °C, alongside a stopwatch accurate to the nearest second and a recording room thermometer permanently placed in the laboratory to monitor ambient conditions throughout the entire test duration.

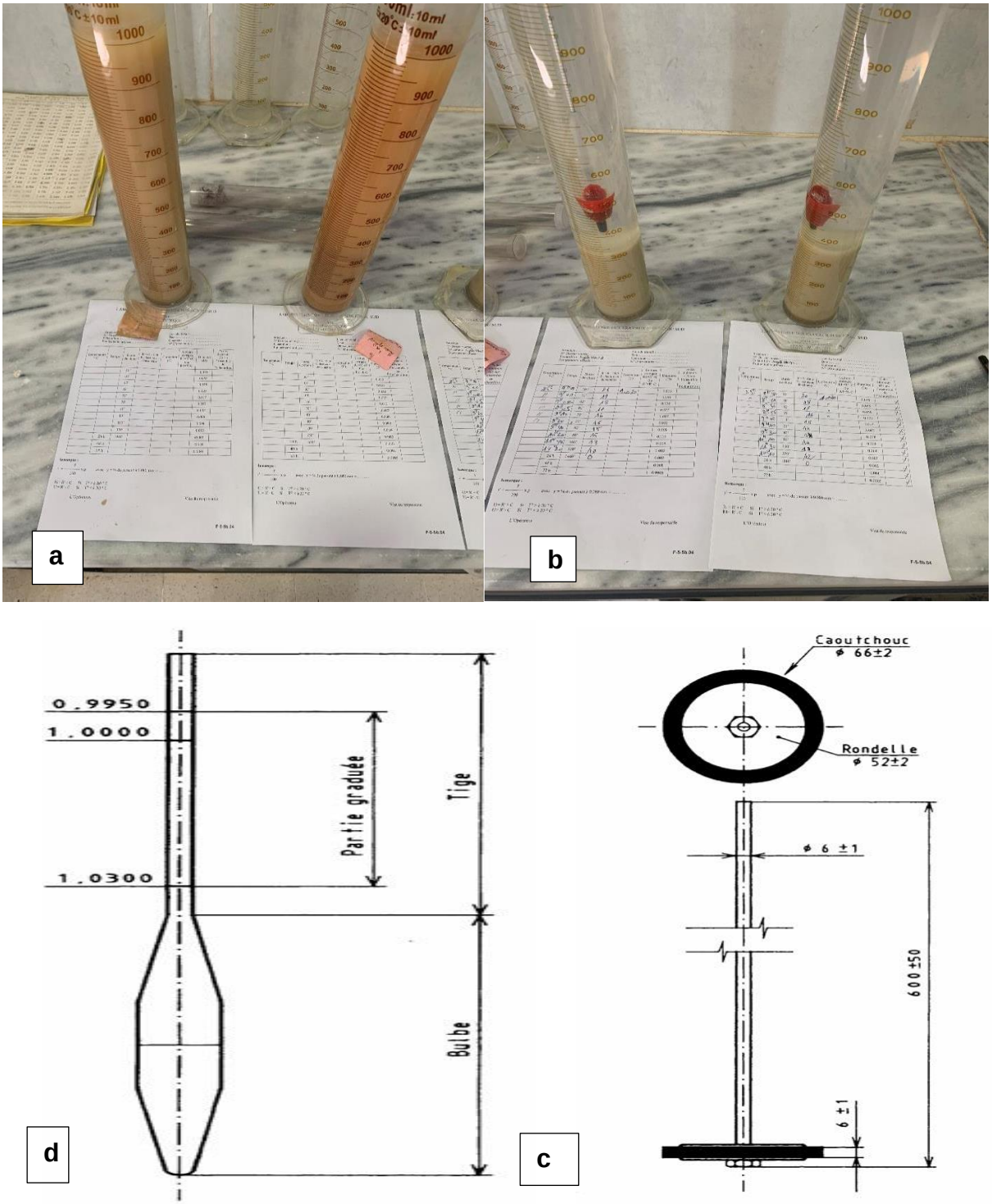

Figure 4: a) Graduated cylinders containing the four clay suspensions during hydrometer sedimentation analysis,; b) Hydrometer immersed in the clay suspension during density measurement;c) Schematic diagram of the manual stirrer (dimensions in mm); d) Schematic diagram of the hydrometer showing the graduated stem and bulb (operating range: 0.9950–1.0300)**.**

II.2.2 : Atterberg Limits Test

The Atterberg limits represent a fundamental measure of the nature and consistency of fine-grained soils, established originally by Albert Atterberg, a Swedish agronomist, and later refined by Arthur Casagrande for geotechnical engineering applications. Depending on its water content, a fine-grained soil may exist in four distinct states — solid, semi-solid, plastic, and liquid — each characterized by different mechanical behaviour and engineering properties, with the boundary between each state defined by a specific limit, as illustrated in Fig. 6a. The objective of this test is to determine the Liquid Limit (LL), the Plastic Limit (PL), and the Plasticity Index (PI) of cohesive fine-grained soils, using a balance, a Casagrande liquid limit device, a grooving tool, mixing dishes, a spatula, and a drying oven.

For the Liquid Limit test, approximately 250 g of air-dried soil is passed through a No. 40 sieve, mixed with water to form a uniform paste (Fig. 6b), and placed into the Casagrande cup where the surface is smoothed to a maximum depth of 8 mm (Fig. 6c). A groove is then cut along the centreline of the soil pat using the grooving tool (Fig. 6d), and the device is cranked at 2 revolutions per second until the groove closes over a distance of 12.7 mm (½ inch), with the number of blows (N) recorded (Fig. 6e, Fig. 6f). When N falls between 15 and 40, the moist soil is collected and weighed (W_2), and after 24 hours of drying the dry mass (W_3) is recorded. This procedure is repeated for a minimum of three trials at varying water contents, and the results are plotted as a flow curve (N versus water content (%)), from which the liquid limit is determined at N = 25.

For the Plastic Limit test, approximately 20 g of dry soil is mixed with water and rolled into small ellipsoidal masses placed between two sheets of filter paper (Fig. 6g). The soil is then rolled until it forms a thread of approximately 3 mm in diameter (Fig. 6h); at this point, if the thread crumbles, the sample is collected and weighed (W_2 and W_3) to determine the corresponding water content, which defines the Plastic Limit. The Plasticity Index is subsequently calculated as the difference between the Liquid Limit and the Plastic Limit ($PI = LL - PL$), providing a key indicator of the plasticity range and clay mineral nature of the tested soil samples.

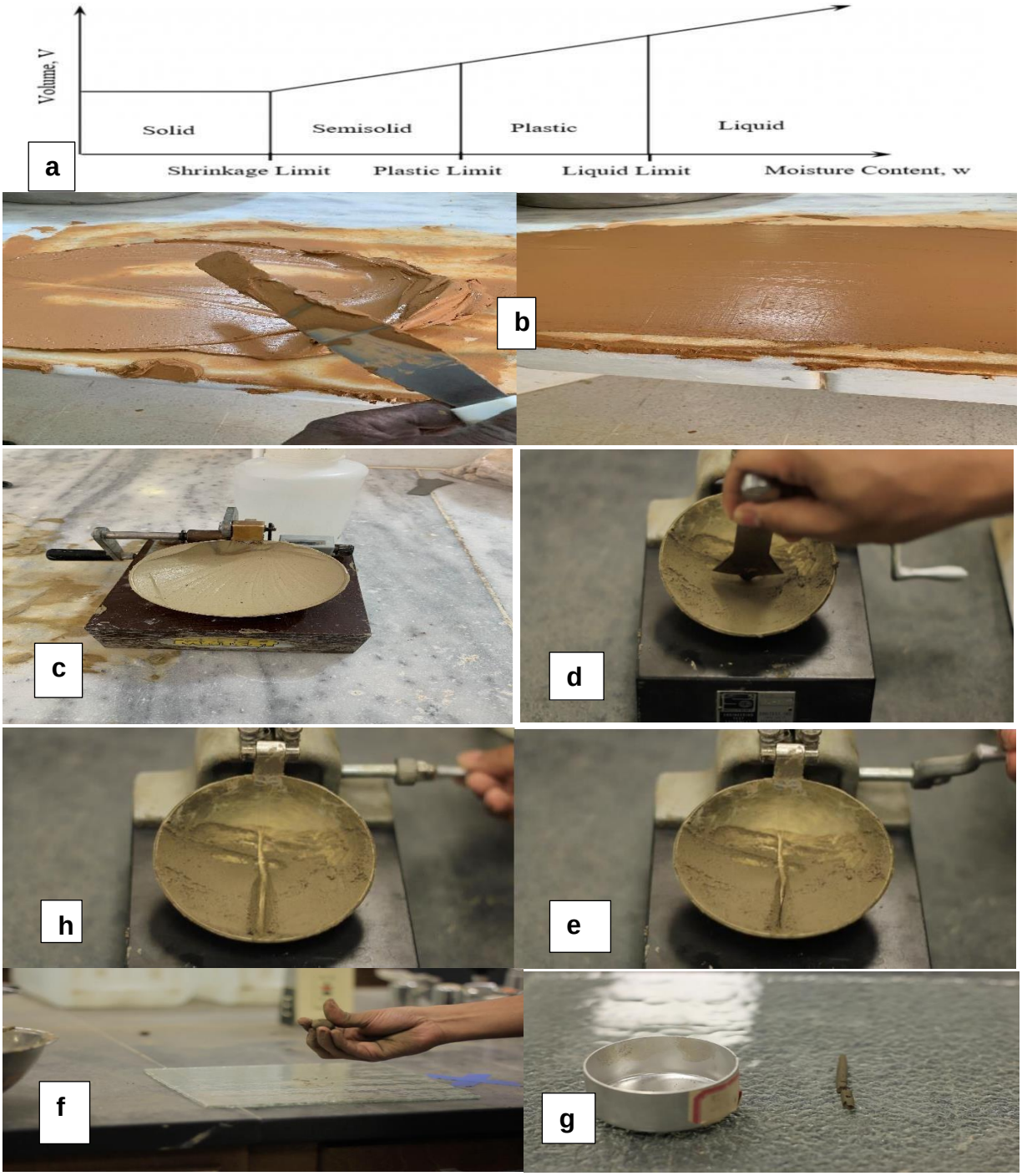

Figure 5: Atterberg limits testing procedure: a) moisture content scale showing the four soil consistency states; b–e) liquid limit determination using the Casagrande apparatus, from slurry preparation to groove closure; f–g) plastic limit determination by the thread-rolling method.

II.2.3 :Bulk & Dry Density (Paraffin Wax Method)

The paraffin wax method for determining bulk and dry density is a careful process designed to give reliable values even for porous or fragile rocks(Fig.7a) . First, the sample is dried in an oven

at 105 ℃ until its mass no longer changes, which ensures that the measurement reflects the true dry state of the material. Then the specimen is coated with paraffin wax (Fig.7b), a protective layer that prevents water from entering the pores during immersion. After this, the sample is weighed in air and then in water, and from these two measurements the real volume of the rock is calculated by hydrostatic principles. The dry density is obtained by dividing the dry mass by this corrected volume, while the bulk density expresses the natural compactness of the rock including its pores and voids. This method is important because it allows engineers to evaluate both the strength and the porosity of materials: high density values indicate compact, durable rocks suitable for construction, while lower values reveal higher porosity and possible weakness. In geotechnical practice, these results are not just numbers but a way to classify materials, to judge their suitability for embankments, foundations, or road layers, and to anticipate how they will behave under load or weathering. In this sense, the paraffin wax method is a simple but powerful tool that connects laboratory measurement with real-world engineering decisions.

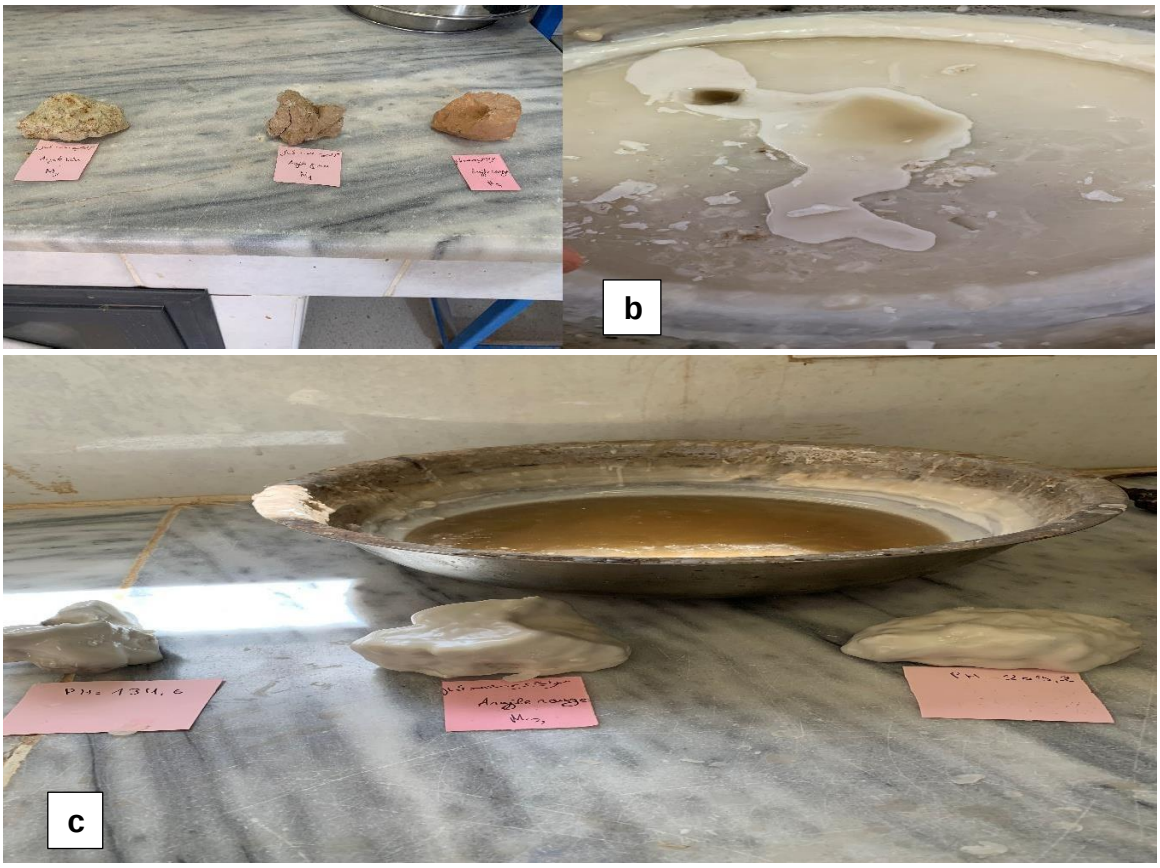

Figure 6: Shows a) the three samples before covering them with wax, b) wax in melting process,c) the three samples after covering them with wax.

II.3: Chemical characterization of four clay samples

II.3.1 : Chloride Test:

The determination of chloride ions soluble in water is an essential chemical test for aggregates, since chlorides can accelerate the corrosion of steel reinforcement in concrete. The procedure begins with a representative sample of 1 kg of aggregate, with particle size not exceeding 20 mm, which is oven-dried at 105–110 °C until constant mass is achieved (Fig.8a). The dried material is crushed, sieved to 600 µm, and quartered to obtain a 100 g portion. This portion is mixed with 200 ml of distilled water and agitated for 24 hours (Fig.8b). After settling, the suspension is filtered, and 25 ml of the filtrate is titrated at neutral pH with silver nitrate ($AgNO_3$), using potassium chromate (K_2CrO_4) as indicator (Fig.8c). A blank test is performed simultaneously to correct for background interference. The endpoint is observed when a brick-red silver chromate precipitate appears, and the chloride content is calculated from the titrant volume, expressed as % Cl^- by mass of dry aggregate. This test, commonly referred to as the Mohr method, provides a reliable measure of chloride contamination in aggregates.

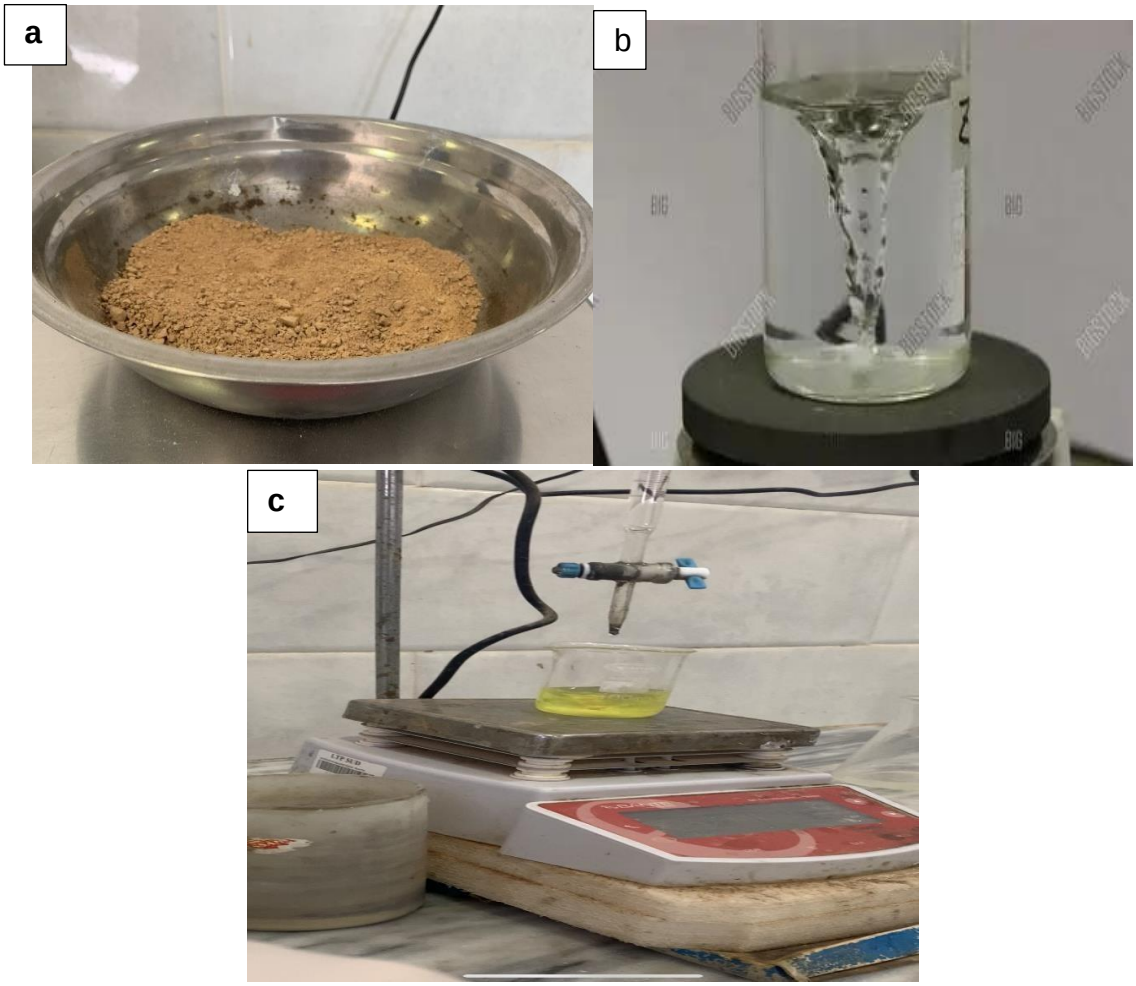

Figure 7: Shows a) Drying, crushing, and sieving of aggregate sample, b) Agitation of sample with distilled water for 24 hours, c) Titration of filtrate with AgNO2 using K2CrO4 indicator.

II.3.2 : Carbonate Test:

The carbonate content test is performed to determine the proportion of calcium carbonate ($CaCO_3$) present in aggregates, which can influence cement hydration and durability. A representative sample of 200 g is first oven-dried at 105–110 °C for 24 to 48 hours (Fig.9a), then cooled in a desiccator. From this, a 0.5 g portion is weighed (mo) after sieving to 425 µm and quartering. The sample is placed in a 100 ml beaker, to which 10 ml of hydrochloric acid (HCl, 1N) is added, along with 2–3 drops of phenolphthalein indicator ($C_{20}H_{14}O_4$, 0.1%). The solution turns red initially, and titration is carried out with sodium hydroxide (NaOH, 1N) until the color change indicates neutralization (Fig.9b). The carbonate content is then calculated from the NaOH volume consumed and expressed as % $CaCO_3$ by mass of aggregate. This test provides a direct measure of carbonate reactivity in aggregates(Fig.9c).

Figure 8: Shows a) Oven-drying of aggregate sample at 105-110 °C, b), c) Titration with NaOH solution showing color change.

II.3.3 : Sulfate Test:

The sulfate test determines the proportion of sulfates in aggregates, which can cause expansion and cracking in concrete. A 200 g sample is oven-dried at 80 °C (or 105–110 °C if necessary) for 48 hours, then cooled in a desiccator (Fig.10a). The dried material is pulverized in a mortar, sieved to 200 µm, and a 1 g portion (Po) is weighed. This is placed in a 250 ml Erlenmeyer flask with 100 ml of 10% hydrochloric acid (HCl), boiled gently for 4–5 minutes, and cooled for 15 minutes (Fig.10b). The solution is filtered through paper No. 541, and the filtrate is diluted to 250 ml with distilled water. From this, 100 ml is taken, and 10 ml of 5% barium chloride ($BaCl_2$) solution is added. The mixture is boiled gently for 5 minutes, cooled for 15 minutes, and filtered again. The filter paper containing the $BaSO_4$ precipitate is placed in a pre-weighed crucible (Pi), calcined at 900 °C for 15 minutes, and re-weighed (P2). The sulfate content is calculated from the mass difference (P2–Pi) and expressed as % SO_4 relative to the dry mass of aggregate. This gravimetric method provides a precise measure of sulfate contamination.

Figure 9: Shows a) Drying, pulverizing, and sieving of aggregate sample, b) Boiling with HCl, cooling, and filtration of solution, c) Precipitation of BaSO4 and calcination in crucible.

II.3.4 : pH Test

The pH test is a simple but informative chemical analysis used to evaluate the reactivity of aggregates and their compatibility with cementitious systems. A representative sample of aggregate is washed with distilled water, and the aqueous extract is collected (Fig.11a). The pH of the extract is then measured using a calibrated pH-meter with sensitivity to 0.1 units (Fig.11b). Most natural aggregates yield slightly alkaline values, typically between 8.0 and 8.5, reflecting the presence of carbonate minerals. A strongly acidic or highly alkaline pH may indicate contamination or unusual mineralogical composition, which could adversely affect cement hydration or promote reinforcement corrosion. The pH test thus serves as a rapid screening tool for aggregate suitability in concrete production.

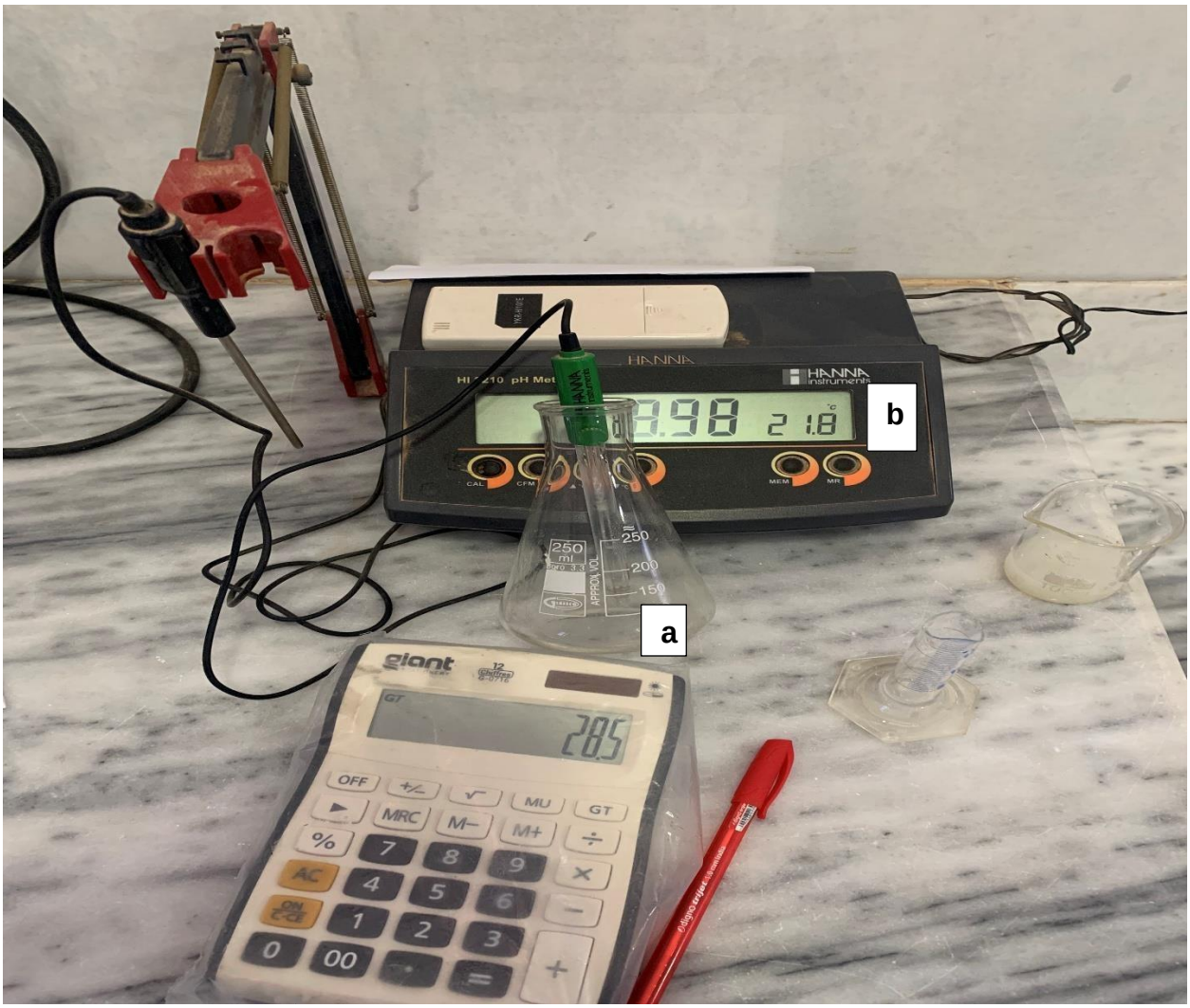

Figure 10. Shows a) Preparation of aqueous extract from aggregate sample, b) Measurement of pH using a calibrated pH-meter.

CHAPTER III: RESULTS AND DISCUSSION

III.1 Introduction

The present chapter synthesises the laboratory results obtained from four clay samples collected in the Timassine region, Wilaya de Tougourt (south-eastern Algeria). The investigated samples red clay, green clay 1, green clay 2, and yellow clay – were subjected to a comprehensive analytical programme encompassing X-ray diffraction (XRD), hydrometer sedimentation analysis, chemical characterisation, and bulk density measurements. The objective is to characterise the mineralogical assemblage, grain-size distribution, physicochemical properties, and physical structure of each clay, and to discuss their implications for geotechnical classification and potential use as construction materials, particularly in fired brick production. The semi-arid context of the Saharan south and the scarcity of local construction materials make this study particularly relevant for regional infrastructure development.

III.2 Mineralogical Analysis by X-ray Diffraction (XRD)

III.2.1 Qualitative Identification of Mineral Phases

X-ray diffraction (XRD) analysis was carried out on the yellow clay sample to determine the crystalline phases present in the bulk material. The diffractogram was recorded over a 5–70° (2θ) range using CuKα radiation (λ = 1.5406 Å). The main identified mineral phases are presented below, and a schematic illustration of the principal diffraction peaks is shown in Figure 12.

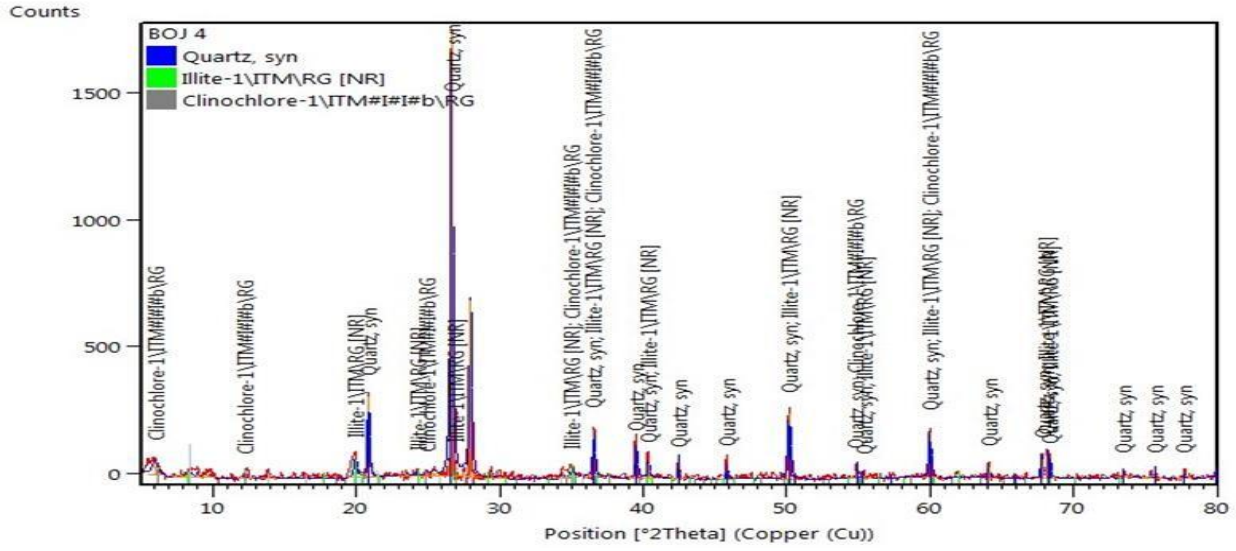

Figure 11. X-ray diffractogram of the yellow clay sample from Timassine. Q = quartz (d = 3.34 Å, 2θ = 26.6°); I = illite; C = clinochlore.

Table 1: Principal mineral phases identified by XRD in the yellow clay sample from Timassine**.**

Mineral Phase	Chemical Formula	Diagnostic Peak (2θ, °)
Quartz	SiO_2	26.6°
Illite	$K_{0.7}Al_2(Si,Al)_4O_{10}(OH)_2$	8.9° / 17.7°
Clinochlore	$Mg_5Al(Si_3Al)O_{10}(OH)_8$	6.2° / 12.5°

III.2.2. Interpretation

Quartz (SiO_2) is the dominant mineral, as indicated by the strongest and most intense diffraction peak centered at 2θ = 26.6°, corresponding to the (101) reflection with a d-spacing of 3.34 Å. The high crystallinity of this phase, reflected by the narrow peak width (low full width at half maximum, FWHM), indicates that quartz occurs as well-ordered coarse to medium silt-sized grains inherited from aeolian and alluvial sediments of the Saharan domain (Chamley, 1989). Quartz provides the mechanical framework and structural rigidity of the clay, reducing plasticity while ensuring dimensional stability during firing (Deer et al., 2013).

Illite ($K_{0.7}Al_2(Si,Al)_4O_{10}(OH)_2$) is identified as a secondary clay mineral. Its characteristic basal reflections at approximately 8.9° (d ≈ 10 Å) and 17.7° (d ≈ 5 Å) are broad and of moderate intensity, consistent with poorly crystalline illite typical of weathered clays formed under arid conditions (Moore & Reynolds, 1997). Illite is a non-expanding 2:1 phyllosilicate in which interlayer potassium ions create strong electrostatic bonding, limiting water uptake and volume changes during wetting and drying cycles (Grim, 1968). Its presence contributes to moderate to low plasticity and is also associated with iron-bearing phases responsible for the yellow-ochre coloration observed macroscopically.

Clinochlore ($Mg_5Al(Si_3Al)O_{10}(OH)_8$), belonging to the chlorite group, is identified as a minor accessory phase. Chlorite minerals are 2:1:1 phyllosilicates characterized by non-expanding interlayers occupied by brucite-like octahedral sheets (Deer et al., 2013). Their presence in Saharan deposits reflects the contribution of mafic rock fragments derived from the Precambrian basement exposed in the Hoggar and Tassili massifs, as reported in regional studies of North African continental sediments (Chamley, 1989). Clinochlore slightly contributes to the plasticity of the material and enhances its thermal stability during firing.

The coexistence of quartz, illite, and clinochlore in the studied clays is consistent with typical mineral assemblages reported in Saharan clays and weathered continental formations ranging from the Mesozoic to Cenozoic in North Africa (Chamley, 1989; Moore & Reynolds, 1997).

III.3. Grain-size distribution by hydrometer sedimentation analysis

Hydrometer sedimentation (densimeter) tests were conducted in accordance with standard procedures to determine the grain-size distribution of the clay fraction (< 0.080 mm) of each sample. The corrected hydrometer readings (R') and the corresponding equivalent particle diameters (D, mm), calculated using Stokes' law, are presented in Tables 3.2 to 3.5. Temperature correction factor C was applied to each series. Figure 13 illustrates the cumulative grain-size distribution curves for all four samples.

The method follows the French standard NF P94-057, which is equivalent to ASTM D7928.[2]

Table 2. Hydrometer sedimentation data – Red Clay (T = 26 °C; C = 1.26).

T (°C)	Time	Duration	R′	Correction C	Diameter D (mm)
26	8h15	30"	21	1.26	0.075
–	8h16	1′	20	–	0.055
–	8h17	2′	20	–	0.038
–	8h20	5′	20	–	0.025
–	8h25	10′	19	–	0.017
–	8h35	20′	17	–	0.012
–	8h55	40′	16	–	0.008
–	9h35	80′	15	–	0.006
–	10h55	160′	15	–	0.004
–	13h35	320′	12	–	0.003
–	24h	1440′	0	–	0.002
–	48h	–	0	–	0.001
–	72h	–	0	–	0.0005

Table 3. Hydrometer sedimentation data – Green Clay 1 (T = 25 °C; C = 1.02).

T (°C)	Time	Duration	R′	Correction C	Diameter D (mm)
25	8h50	30"	20	1.02	0.075
–	8h51	1′	18	–	0.055
–	8h52	2′	17	–	0.038
–	8h55	5′	16	–	0.025
–	9h00	10′	15	–	0.017
–	9h10	20′	14	–	0.012
–	9h30	40′	15	–	0.008
–	10h10	80′	14	–	0.006
–	13h00	160′	13	–	0.004
–	14h10	320′	12	–	0.003
–	24h	1440′	0	–	0.002
–	48h	–	0	–	0.001
–	72h	–	0	–	0.0005

Table 4. Hydrometer sedimentation data – Green Clay 2 (T = 25 °C; C = 1.02).

Temp. (°C)	Time	Duration	R’	Correction (C)	Diameter (D, mm)
2.5	9h00	30″	21	1.02	0.075
	9h01	1′	19	—	0.055
	9h02	2′	18	—	0.038
	9h05	5′	17	—	0.025
	9h10	10′	16	—	0.017
	9h20	20′	15	—	0.012
	9h40	40′	15	—	0.008
	10h20	80′	15	—	0.006
	11h40	160′	13	—	0.004
	14h20	320′	10	—	0.003
	24h	1440′	0	—	0.002
	48h	—	0	—	0.001
	72h	—	0	—	0.0005

Table 5. Hydrometer sedimentation data – Yellow Clay (T = 27 °C; C = 1.51).

T (°C)	Time	Duration	R′	Correction C	Diameter D (mm)
27	8h20	30"	15	1.51	0.075
–	8h21	1′	15	–	0.055
–	8h22	2′	14	–	0.038
–	8h25	5′	14	–	0.025
–	8h30	10′	13	–	0.017
–	8h40	20′	12	–	0.012
–	9h00	40′	12	–	0.008
–	9h40	80′	11	–	0.006
–	11h00	160′	10	–	0.004
–	13h40	320′	9	–	0.003
–	24h	1440′	0	–	0.002
–	48h	–	0	–	0.001
–	72h	–	0	–	0.0005

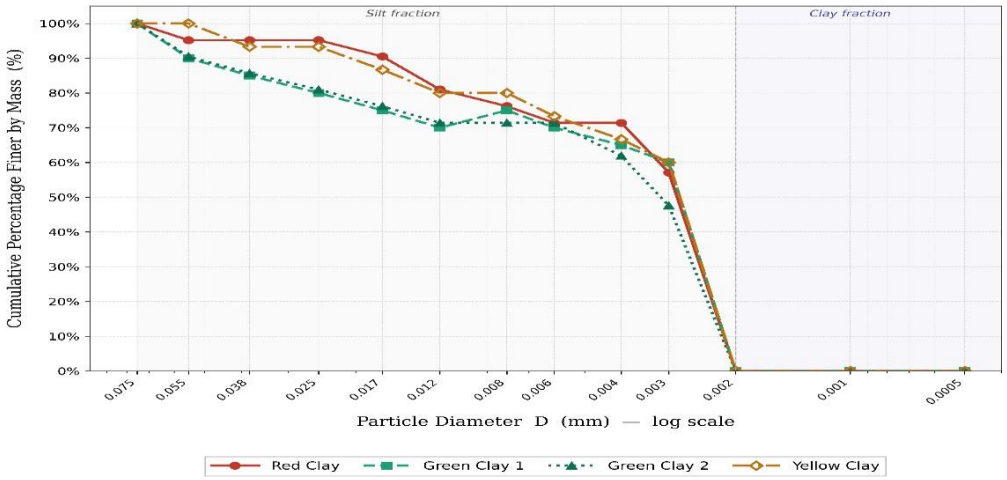

Figure 12. Cumulative grain-size distribution curves derived from hydrometer sedimentation tests for the four Timassine clay samples.

III.3.1 Discussion of Grain-Size Results

The sedimentation data reveal systematic differences in the textural character of the four clays. Red clay exhibits the highest initial R′ values (~21 at D = 0.075 mm), indicating the greatest proportion of coarser silt-sized particles at the onset of sedimentation, with a gradual decline to zero at D = 0.002 mm over 24 hours. This graded distribution reflects a heterogeneous, poorly sorted sediment in which fine sands and coarse silts coexist with clay-sized particles. The coarser fraction provides inter-grain friction and may enhance compressive strength in fired products but reduces workability during plastic forming (Folk & Ward, 1957).

Green Clay 1 displays a smoother and steeper sedimentation curve, with R′ declining from 20 to 0 more uniformly. This behaviour reflects a better-sorted, predominantly silt-to-clay fraction with fewer coarse particles, conferring higher plasticity and greater homogeneity. Green Clay 2 is texturally similar but slightly finer, as evidenced by the more rapid initial drop and lower final R′ value at D = 0.003 mm (R′ = 10 compared to 12 for Green Clay 1). These observations suggest that Green Clay 2 is richer in the true clay fraction (< 0.002 mm), which can increase shrinkage but enhances green strength and compaction during moulding (Tanner, 2003).

Yellow clay stands apart as the finest material. Its low initial R′ value (15 at D = 0.075 mm) and steady decline to R′ = 9 at D = 0.003 mm indicate an overwhelming dominance of fine particles throughout the test duration. The homogeneity and fineness of this sample correlate with its XRD-identified mineral assemblage (illite + clinochlore), confirming that the high specific surface area of these phyllosilicates concentrates the measured hydrometer response at small diameters (Moore & Reynolds, 1997). The high plasticity index implied by this grain-size distribution is consistent with the smooth tactile texture observed in the field, a typical feature of clay-rich, fine-grained sediments in arid continental environments (Grim, 1968; Mitchell & Soga, 2005).

III.4 Chemical and Physicochemical Characterisation

Chemical analyses were conducted to determine the contents of soluble salts (sulfates and chlorides), calcium carbonate, insoluble residue, and pH in each clay sample. These parameters are essential for evaluating the suitability of the clays for fired brick production, as excessive concentrations of soluble salts may lead to efflorescence, subflorescence, and surface defects during drying and firing processes. The analytical results are summarized in Table 6.

Table 6. Chemical and physicochemical characteristics of the four Timassine clay samples.

Sample	% Insolubles	% SO_3^{2-}	% SO_4^{2-}	% $CaCO_3$	% Cl^-	pH
Red Clay	100.0	34.30	41.20	15.80	0.03	8.30
Green Clay 1	100.0	34.30	41.20	19.80	0.05	8.35
Green Clay 2	100.0	34.30	41.20	19.80	0.06	8.30
Yellow Clay	100.0	34.30	41.20	19.40	0.09	8.31

3.4.1 Insoluble Residue

All four samples record 100% insoluble residue, confirming that the materials are entirely composed of non-soluble mineral phases (quartz, clay minerals, carbonates). This result is consistent with the XRD findings and indicates that no soluble silicates or reactive aluminosilicates are present. A high insoluble fraction is generally favourable for structural brick applications as it ensures dimensional stability and limits excessive sintering reactions at firing temperatures (Grim, 1968).

3.4.2 Sulfate Content

All samples exhibit identical and notably elevated sulfate concentrations, with SO_4^{2-} at 41.20% and SO_3^{2-} at 34.30%. These values significantly exceed the threshold of 0.50% commonly cited as the upper safe limit for ceramic-grade clays. The uniformly high sulfate content across all four samples suggests a regional geochemical signature rather than localised contamination, likely linked to the evaporitic character of the Saharan subsoil, where gypsum ($CaSO_4 \cdot 2H_2O$) and anhydrite ($CaSO_4$) are common diagenetic minerals within Cretaceous continental red beds (Dondi et al., 1997).

During brick firing, soluble sulfates migrate to the surface during drying and subsequently crystallise upon cooling, producing white saline efflorescence. In severe cases, sub-surface crystal growth generates internal stresses capable of causing surface spalling and structural degradation. Mitigation strategies include the addition of barium carbonate ($BaCO_3$) as a sulfate scavenger, or blending with low-sulfate materials to dilute the soluble fraction (Dondi et al., 1997)

3.4.3 Calcium Carbonate Content

Calcium carbonate contents vary between 15.80% (red clay) and 19.80% (green clays 1 and 2). These values are moderate for North African clays but remain above the critical threshold of approximately 10%, above which calcite decomposition during firing ($CaCO_3 \rightarrow CaO + CO_2$ at

~900 °C) may produce reactive free lime (CaO). Upon re-exposure to atmospheric moisture, CaO hydrates to $Ca(OH)_2$, generating expansive forces that cause surface popping and cracking in fired bricks (Cultrone et al., 2004). Red clay, with the lowest carbonate content (15.80%), is least susceptible to this phenomenon, while the green clays require careful temperature management during firing to minimise calcite decomposition (Cultrone et al., 2004; Dondi et al., 1997).

3.4.4 Chloride Content and pH

Chloride concentrations are low for all samples, ranging from 0.03% (red clay) to 0.09% (yellow clay), remaining well below the 0.20% limit beyond which significant salt damage is expected (Dondi et al., 1997). The slightly elevated chloride in yellow clay is consistent with its finer grain size and greater specific surface area, which adsorbs mobile ions preferentially (Bergaya et al., 2006). All samples are mildly alkaline (pH 8.30–8.35), reflecting the calcareous mineralogy and the arid-evaporitic soil environment. The alkaline pH is conducive to the stability of illite and inhibits the dissolution of silicates, which is a positive indicator for material durability (Grim, 1968; Mitchell & Soga, 2005).

III.5 Bulk and Dry Density Analysis

The wet bulk density (ρh) of the clay samples was determined using the paraffin-coated hydrostatic weighing method, which is widely applied for irregularly shaped soil aggregates (Mitchell & Soga, 2005). This method consists of coating the sample with a thin layer of paraffin ($\rho_{paraffin} = 0.9$ g/cm³) and measuring the apparent weight loss in water in order to determine the total displaced volume. The paraffin volume is then subtracted from the gross volume to obtain the net sample volume. The results are presented in Table 7.

Table 7 . Bulk density measurements of clay samples by the paraffin hydrostatic method.

Sample	Wet Wt. (g)	Paraf. Wt. (g)	Paraf. ρ (g/cm³)	Wt. in Water (g)	Gross Vol. (cm³)	Paraf. Vol. (cm³)	Net Vol. (cm³)	ρh (g/cm³)
Yellow Clay	134.6	25.5	0.9	62.5	98.6	28.3	70.3	1.91
Green Clay	209.2	28.3	0.9	93.5	144.0	31.4	112.6	1.85
Red Clay	246.0	35.6	0.9	115.5	166.1	39.5	126.6	1.94

III.5.1 Discussion of Density Results

Red clay records the highest wet bulk density (ρh = 1.94 g/cm³), indicating greater compactness and relatively lower porosity compared to the other samples. This behaviour is consistent with its coarser grain-size distribution, where a broader range of particle sizes allows finer particles to fill the voids between coarser grains, thereby improving packing efficiency (Mitchell & Soga, 2005). Higher bulk density is generally associated with improved mechanical performance in fired brick products, including increased compressive strength and reduced water absorption (Grim, 1968; Cultrone et al., 2004).

Yellow clay exhibits an intermediate wet bulk density (ρh = 1.91 g/cm³), despite being the finest-grained material among the three samples. This behaviour may be attributed to the preferred orientation and dense stacking of platy illite particles during natural consolidation, which progressively reduces interparticle void space (Bergaya et al., 2006). However, this particle fabric is structurally metastable and can be readily disrupted upon hydration, leading to swelling, loss of cohesion, and a significant reduction in bearing capacity.

Green clay shows the lowest wet bulk density (ρh = 1.85 g/cm³) and the largest net volume (112.6 cm³), indicating the greatest relative porosity among the three samples. This is consistent with its intermediate grain-size distribution: it lacks a sufficient coarse fraction to bridge macropores and an insufficient clay fraction to achieve dense particle packing (Mitchell & Soga, 2005). In geotechnical terms, elevated porosity is associated with increased compressibility, higher void ratio, and reduced shear strength under applied load parameters that must be carefully evaluated in foundation design and earthwork applications in the Tougourt region (Bergaya et al., 2006; LCPC/SETRA, 2000).

III.6. ATTERBERG LIMITS

III.6 .1 Results

The consistency limits of the four clay samples from the Timassine region were determined in accordance with the French standard NF P 94-051, which specifies the procedures for the determination of the liquid limit (WL) by the Casagrande percussion cup method and the plastic limit (WP) by the thread-rolling method. The plasticity index (IP) was subsequently calculated as the difference between WL and WP (IP = WL − WP). The results are summarised in Table .8, and the positions of each sample on the Casagrande plasticity chart are presented in Figure 14.

Table 8. Atterberg limits of the four Timassine clay samples (NF P 94-051).

Sample	Liquid Limit WL (%)	Plastic Limit WP (%)	Plasticity Index IP (%)	Casagrande Classification
Red Clay (M3)	67.16	23.67	43.49	Highly plastic clay (CH)
Green Clay 1	72.32	30.80	41.52	Highly plastic clay (CH)
Green Clay 2	72.48	31.43	41.05	Highly plastic clay (CH)
Yellow Clay	62.87	29.52	33.35	Highly plastic clay (CH)

III.6.2 Discussion

III.6.2.1. Liquid Limit

The liquid limit values range from 62.87% (yellow clay) to 72.48% (green clay 2), indicating that all four samples require a substantial addition of water before transitioning from the plastic to the liquid state. These elevated WL values are consistent with the predominance of illite and clinochlore identified by XRD analysis, as these phyllosilicate minerals possess high specific surface areas and significant inter-layer water retention capacity (Mitchell & Soga, 2005; Bergaya et al., 2006).

The two green clays exhibit nearly identical liquid limits (72.32% and 72.48% respectively), confirming their close mineralogical and textural affinity already observed in both the XRD and grain-size analyses. Their high WL values reflect a clay fraction with a strong capacity to adsorb water within the double diffuse layer surrounding each clay particle, a property governed by the surface charge density and exchangeable cation content of the illitic minerals (Grim, 1968).

Red clay, despite its coarser grain-size distribution, records a high liquid limit of 67.16%, reflecting the contribution of its clay mineral fraction particularly the fine illitic component to overall water retention. Yellow clay displays the lowest WL (62.87%) among the four samples. Although it is the finest-grained material, its comparatively lower liquid limit may be attributed to the specific interlayer bonding characteristics of its illite-clinochlore assemblage, which restricts inter-particle water retention relative to the green clays (Bergaya et al., 2006).

III.6.2.2. Plastic limit

The plastic limit values range from 23.67% (red clay) to 31.43% (green clay 2). Red clay displays a markedly lower WP compared to the other three samples, indicating a narrow moisture range over which the material exhibits plastic behaviour. This is consistent with its coarser grain-

size distribution and lower clay mineral content relative to the finer samples: the lower specific surface area of the coarser fraction reduces the cohesive interparticle forces that sustain plasticity at lower moisture contents (Mitchell & Soga, 2005).

In contrast, the green clays and yellow clay exhibit comparable plastic limit values (29.52–31.43%), reflecting similar interparticle cohesion characteristics in the plastic state. This convergence is governed by the shared illitic mineralogy of these three samples, whose platy particle morphology and negative surface charge generate equivalent cohesive bonding at the plastic–solid boundary (Grim, 1968).

III.6.2.3. Plasticity index and Casagrande classification

The plasticity index values range from 33.35% (yellow clay) to 43.49% (red clay), placing all four samples above the A-line of the Casagrande plasticity chart, defined by the equation IP = 0.73(WL − 20), and beyond the WL = 50% threshold. This positions all samples firmly within the highly plastic clay (CH) domain of the USCS classification, confirming a high shrink–swell potential and significant geotechnical sensitivity (LCPC/SETRA, 2000).

Red clay records the highest plasticity index (IP = 43.49%), a result that may appear inconsistent with its coarser grain-size distribution. This apparent contradiction is resolved by examining the plastic limit: the markedly low WP of 23.67% generates a wide plasticity range despite a moderate liquid limit, producing the highest IP value among the four samples. This behaviour is characteristic of illitic fine fractions that become cohesive at relatively low moisture contents (Mitchell & Soga, 2005). The very low WP of red clay also implies that this material transitions rapidly from a plastic to a solid, brittle state upon drying a characteristic with direct implications for brick drying management, as uncontrolled moisture loss may generate significant tensile stresses and surface cracking.

The green clays exhibit closely matched plasticity indices (IP = 41.52% for Green Clay 1 and IP = 41.05% for Green Clay 2), confirming their mineralogical and textural similarity. Their positions on the Casagrande chart well above the A-line and at WL > 70% indicate a clay fraction with very high water affinity, significant volume change potential upon wetting and drying, and elevated compressibility under load (Bergaya et al., 2006; LCPC/SETRA, 2000).

Yellow clay records the lowest plasticity index (IP = 33.35%), attributable to its comparatively higher plastic limit (WP = 29.52%), which narrows the plasticity range relative to the other samples. Despite being the finest-grained material, its lower IP suggests that the specific clay mineral assemblage (illite + clinochlore) in this sample provides less cohesive bonding per unit of moisture content than the green clay assemblages. Nevertheless, its position on the Casagrande chart remains firmly within the CH domain, confirming the risk of significant volume change under seasonal moisture fluctuations.

a

RAPPORT D'ESSAI
Limites d'Atterberg
NF P 94 - 51

Client :
Projet :
Endroit :

N° Projet :
Réf. Client :
N° rapport : Rév :

Echantillon n° : Argile rauge M3
Sondage n° :
Profondeur :
Matériaux :

Provenance :
Endroit de prélèvement :
Prélevé par : Reçu le :
Date prélèvement : Date essais :

Limite de Liquidité (%) : WL = 67,16
Limite de Plasticité (%) : WP = 23,67
Indice de Plasticité (%) : IP = 43,49

Teneur en eau naturelle (%) : Weau =

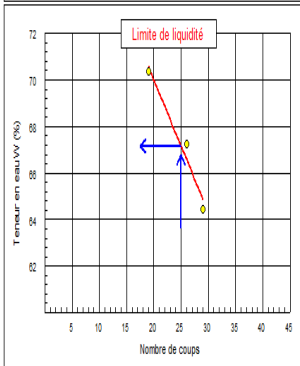

Limite de plasticité

Ech N°	W (%)
1	23,67

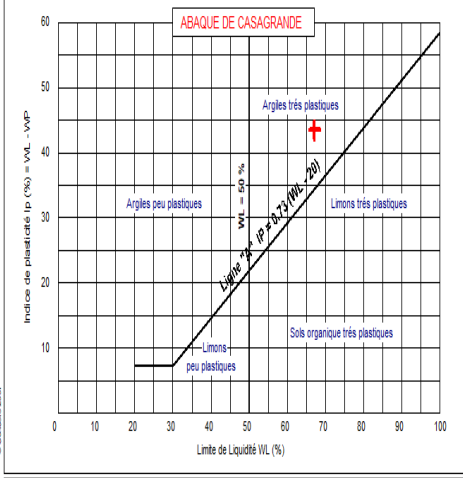

Remarque :

Préparé par : Date :
Approuvé par : Date :

b

RAPPORT D'ESSAI
Limites d'Atterberg
NF P 94 - 51

Client :
Projet :
Endroit :

N° Projet :
Réf. Client :
N° rapport : Rév :

Echantillon n° : Argile vers 1
Sondage n° :
Profondeur :
Matériaux :

Provenance :
Endroit de prélèvement :
Prélevé par : Reçu le :
Date prélèvement : Date essais :

Limite de Liquidité (%) : WL = 72,32
Limite de Plasticité (%) : WP = 30,80
Indice de Plasticité (%) : IP = 41,52

Teneur en eau naturelle (%) : Weau =

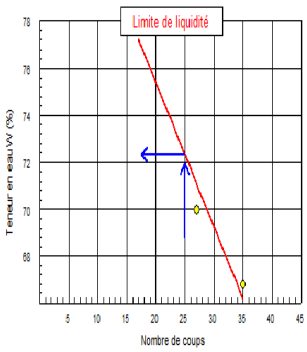

Limite de plasticité

Ech N°	W (%)
1	30,8

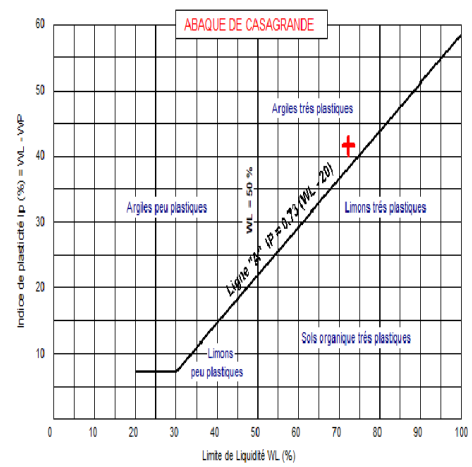

Remarque :

Préparé par : Date :
Approuvé par : Date :

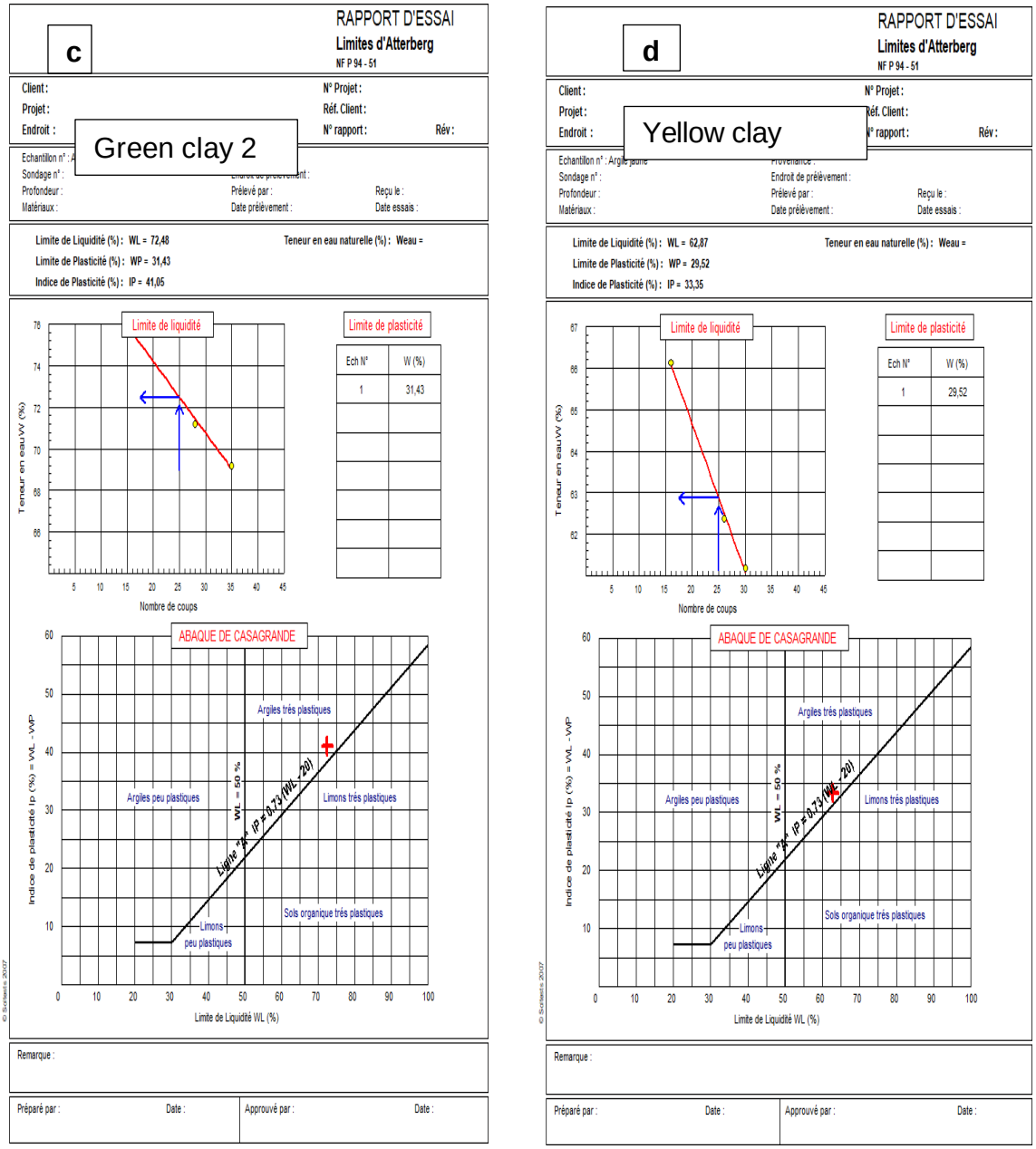

Figure 13: shows Atterberg limits of a) Red Clay (M3) b) green clay 1, c) green clay 2, d) yellow clay : liquid limit curve and Casagrande plasticity chart position (NF P 94-051). WL = 67.16%; WP = 23.67%; IP = 43.49% (CH — highly plastic clay).

III.7. Geotechnical Classification and Engineering Implications

Based on the combined grain-size, mineralogical, density, and Atterberg limit data, the Timassine clays can be classified within the Unified Soil Classification System (USCS) and the French GTR framework (LCPC/SETRA, 2000). The predominantly silt-clay textural character of all four samples, combined with the moderate-to-high plasticity confirmed by Atterberg limit testing (IP ranging from 33.35% to 43.49%), places them unambiguously in the CH (highly plastic clay) category according to the Casagrande classification. Red clay, with its coarser grain-size distribution and highest plasticity index (IP = 43.49%), may exhibit transitional CL–CH behaviour under field compaction conditions; yellow clay, with its fine texture, high illite content, and IP of 33.35%, also falls within the CH domain (Mitchell & Soga, 2005).

In geotechnical engineering practice, CL clays present moderate sensitivity to moisture changes and exhibit reasonable shear strength when compacted to optimum moisture content. CH clays are more problematic: they exhibit high shrink–swell potential, low permeability, and pronounced sensitivity to wetting–drying cycles (Mitchell & Soga, 2005; Grim, 1968). Both categories require careful site investigation and ground treatment including lime stabilisation and compaction control before use as subgrade or fill material in road construction or building foundations. Given the semi-arid climate of the Tougourt region, where intense episodic rainfall alternates with prolonged drought periods, the cyclic wetting and drying of expansive clay layers constitutes a significant geohazard that must be systematically evaluated in any infrastructure project (LCPC/SETRA, 2000).

III.7.1. Assessment for Fired Brick Production

From the perspective of ceramic raw material suitability, red clay emerges as the most balanced candidate for fired brick manufacturing. Its moderate carbonate content (15.80%), lowest chloride concentration (0.03%), highest wet bulk density (1.94 g/cm³), and coarser texture collectively suggest that fired bricks produced from red clay would exhibit acceptable compressive strength, limited efflorescence, and manageable drying shrinkage (Cultrone et al., 2004). Nevertheless, the uniformly elevated sulfate content (SO_4^{2-} = 41.20%) recorded across all samples represents the most critical technological constraint and necessitates corrective blending or chemical treatment notably through the addition of barium carbonate ($BaCO_3$) as a sulfate scavenger regardless of which clay is selected for production (Dondi et al., 1997).

The green clays offer intermediate workability and plasticity, making them suitable as blending components to improve the cohesiveness of coarser red clay mixes. Their higher carbonate contents (19.80%) require that firing temperatures be carefully controlled below approximately 850 °C to prevent calcite decomposition and the associated risk of free lime formation (Cultrone et al., 2004). Yellow clay, despite its smooth texture and moderate plasticity (IP = 33.35%), presents the most challenging chemical and mechanical profile: elevated carbonate

and chloride contents combined with a high liquid limit (WL = 62.87%) make it prone to cracking during drying and susceptible to efflorescence upon firing (Dondi et al., 1997; Bergaya et al., 2006). Its best use is therefore as a minor plasticising additive at proportions not exceeding 20 wt.% in a clay blend dominated by red or green clay.

GENERAL CONCLUSION

This study focused on the characterization of clays collected from the Timassine region in Touggourt, northeastern Sahara.

The geological framework shows that the area belongs to the Saharan platform, with formations from the Cretaceous to the Quaternary. These deposits explain the presence of clay horizons that were analyzed in this work.

The laboratory methods applied X-ray diffraction, hydrometer sedimentation, chemical tests, bulk density, and Atterberg limits allowed a complete description of the four clay samples (red, green 1, green 2, and yellow). The results revealed that quartz, illite, and clinochlore are the main minerals. Grain-size analysis showed differences between coarser red clay and finer yellow clay. Chemical tests highlighted very high sulfate contents, moderate carbonate levels, and slightly alkaline pH. Density and Atterberg limits confirmed that all samples belong to the category of highly plastic clays (CH).

From a practical point of view, these clays can be used in construction, especially for fired bricks. Red clay appears the most balanced, but the high sulfate content in all samples remains a serious problem that requires treatment or blending.

In conclusion, the Timassine clays are important local resources. Their study shows the link between geology, mineralogy, and geotechnical properties, and underlines the need for careful management before use. This work contributes to a better understanding of Saharan clays and supports their sustainable use in regional development.

REFERENCES

Bel, A., & Cuche, D. (1969). *Étude géologique du Sahara algérien.* Algiers: Centre de Recherches Sahariennes. *Ouvrage ancien.*

Bergaya, F., Theng, B. K. G., & Lagaly, G. (2006). *Handbook of Clay Science.* Developments in Clay Science, Vol. 1. Elsevier. ISBN: 978-0-08-044183-2

Bouzouada, M., & Boussaid, A. (2018). Continental Terminal deposits in the Algerian Sahara. *Journal of African Earth Sciences, 145*, 123–135.https://doi.org/10.1016/j.jafrearsci.2018.05.010

Busson, G. (1972). *Stratigraphie et sédimentation du Sahara nord oriental.* Paris: Centre National de la Recherche Scientifique (CNRS).

Chamley, H. (1989). *Clay Sedimentology.* Springer. https://doi.org/10.1007/978-3-642-85916-8

Cultrone, G., Sebastián, E., & de la Torre, M. J. (2005). Mineralogical and physical behaviour of solid bricks with additives. *Construction and Building Materials, 19*(1), 39–48. https://doi.org/10.1016/j.conbuildmat.2004.04.035

Deer, W. A., Howie, R. A., & Zussman, J. (2013). *An Introduction to the Rock-Forming Minerals* (3rd ed.). Mineralogical Society. ISBN: 978-0-903056-27-4

Dondi, M., Marsigli, M., & Fabbri, B. (1997). Recycling of industrial and urban wastes in brick production: A review. *Tile & Brick International, 13*(3), 218–225.

Fabre, J. (1976). *Lithostratigraphie et sédimentation du Crétacé inférieur du Sahara.* Paris: CNRS.

Folk, R. L., & Ward, W. C. (1957). Brazos River bar: A study in the significance of grain size parameters. *Journal of Sedimentary Research, 27*(1), 3–26. https://doi.org/10.1306/74D70646-2B21-11D7-8648000102C1865D

Grim, R. E. (1968). *Clay Mineralogy* (2nd ed.). McGraw-Hill. ISBN: 978-0-07-024832-2

LCPC/SETRA. (2000). *Guide Technique Routier (GTR) : Classification des matériaux utilisables en construction routière.* Laboratoire Central des Ponts et Chaussées. *Document technique officiels.*

Mitchell, J. K., & Soga, K. (2005). *Fundamentals of Soil Behavior* (3rd ed.). Wiley. ISBN: 978-0-471-46302-7

Moore, D. M., & Reynolds, R. C. (1997). *X-Ray Diffraction and the Identification and Analysis of Clay Minerals* (2nd ed.). Oxford University Press. ISBN: 978-0-19-508713-0

NF P94-051. (1995). *Détermination des limites d'Atterberg.* Association Française de Normalisation (AFNOR).

Tanner, W. F. (2003). *Coarse-Grained Sediments: Depositional Systems and Facies.* Gulf Coast Section SEPM Foundation.